IOP Conf. Series: Journal of Physics: Conf. Series **1489** (2020) 012012 doi:10.1088/1742-6596/1489/1/012012

Dynamical Analysis of Chemostat Model Incorporated with Substrate Inhibition and Variable Yield Coefficient

U A F M Sadiq[1], S S Jamaian[1,*] and H M Safuan[1]

[1]Department of Mathematics and Statistics, Faculty of Applied Sciences and Technology, Universiti Tun Hussein Onn Malaysia, Pagoh Educational Hub, 84600 Pagoh, Johor, Malaysia

E-mail: *suhana@uthm.edu.my

Abstract. This paper analyses a chemostat model for microbial production by considering substrate inhibition and variable yield coefficient. The Andrews growth model is considered to describe the inhibitory effect of high substrate concentration towards the microbial growth. The dependency of product yield towards the substrate concentration also incorporated in the chemostat model. The stability and bifurcation analyses of the chemostat model are presented to investigate the dynamical behaviour of microbial in the chemostat and to identify the parameter region that generates oscillations in the chemostat. The steady state solutions and their stability are determined as a function of residence time. When the feed substrate concentration is adjusted to be more than 6.1 g/L, there exist a parameter range of residence time that improves the microbial production in the chemostat.

1. Introduction

In recent years, the demand for microbial products such as vitamins, antibiotics, biofuel, vaccines and pharmaceutical drugs has gained the interest of researches. Hence, in order to fulfil these demands, the production of the microbial needs to be improved by understanding the mechanism of microbial growth which can be studied using an experimental apparatus called continuous stirred tank reactor (CSTR) or chemostat. Chemostat is a tool that has been widely used for continuous production of cell mass or microbial over an indefinite period.

The chemostat can be effectively functioned for microbial growth by understanding the growth rate of microbial in the reactor which can be described by the growth rate models. Hence, the growth rate model plays an important role in the production of microbial in the chemostat. Previously, different types of growth models such as Monod [1], Tessier [2] and Contois [3] models was considered when analyzing the chemostat model with variable yield coefficient. These models represent the growth of microbial based on the substrate concentration which means the higher the substrate concentration, the higher the growth rate of microbial.

However, in real – life situation there exist some substrates that will inhibit microbial growth at a high concentration of substrate. Therefore, a substrate inhibition model called as Andrews growth model is considered to estimate the growth of microbial in chemostat. Andrews [4] growth kinetics model is an extension of Monod model where an additional substrate inhibition term has been included. This model has been widely used for many applications since it provided a good fit to the experimental data especially for wastewater treatment systems [5–14].

Some experimental studies of chemostat have found that microbial population in the chemostat shows oscillatory behavior which alter the stability of the system. It is found that this behavior occurs due to the dependency of the yield coefficient on the substrate concentration [15,16]. Hence, the yield coefficient should not be assumed as a constant. A number of theoretical studies have been done to study the consequence of this assumption [17–21]. It is proved that by considering the variable yield coefficient, bifurcation occur to the system which alter the stability of the system and hence can improve the production of microbial.

Therefore, in this research the chemostat model with variable yield coefficient and Andrews growth model is analyzed in order to accurately explains the growth of microbial in the chemostat. The dynamical behaviors of the model are discussed by obtaining the steady state solutions. The condition for washout of cell mass in the reactor to occur, the conditions for the cell mass in the reactor is maximized and the condition for oscillation of microbial to occur is determined by investigating the stability and bifurcation analyses.

2. Mathematical Model of Chemostat

The microbial system in chemostat, in which cell mass of microbial, X grows by consuming substrate, S will be investigated in this study. The microbial growth rate is estimated using the Andrews growth model and the variable yield coefficient is considered.

2.1. Dimensional chemostat model

The mathematical model for microbial in chemostat can be described as

$$\frac{\mathrm{d}X}{\mathrm{d}t} = \mu_{\max} SX\left(K_S + S + \frac{S^2}{K_I}\right)^{-1} + \frac{1}{\tau}\left(X_0 - X\right), \tag{1a}$$

$$\frac{\mathrm{d}S}{\mathrm{d}t} = \frac{(S_0 - S)}{\tau} - \frac{\mu_{\max} SX}{(\alpha + \beta S)}\left(K_S + S + \frac{S^2}{K_I}\right)^{-1}, \tag{1b}$$

where X is the cell mass concentration, X_0 is the initial substrate concentration, S is the substrate concentration, S_0 is the initial substrate concentration, t is the time, $\frac{\mathrm{dX}}{\mathrm{d}t}$ is the rate of change of cell mass, $\frac{\mathrm{dS}}{\mathrm{d}t}$ is the rate of change of substrate, $\tau = V / F$ is the residence time, V is the volume of the mixture, F is the flow rate, $\mu_{\max}$ is the maximum specific growth rate, K_S is the saturation constant and K_I is the inhibition constant, α and β are constant in yield coefficient.

2.2. Dimensionless chemostat model

The dimensionless variables for substrate concentration (S), cell mass concentration (X) and time (t) are introduced as follows

$$S = S^* K_S, \tag{2}$$

$$X = \alpha X^* K_S, \tag{3}$$

$$t = t^* \left(\mu_{\max}\right)^{-1}. \tag{4}$$

The dimensionless chemostat model is obtained by substituting equation (2), equation (3) and equation (4) into equation (1a) and equation (1b) which is written as

$$\frac{\mathrm{d}X^*}{\mathrm{d}t^*} = \left(S^*X^*\right)\left(1+S^*+I\left(S^*\right)^2\right)^{-1} + \left(X_0^*-X^*\right)\left(\tau^*\right)^{-1}, \tag{5a}$$

$$\frac{\mathrm{d}S^*}{\mathrm{d}t^*} = \left(S_0^*-S^*\right)\left(\tau^*\right)^{-1} - \left(S^*X^*\right)\left(\left(1+S^*+I\left(S^*\right)^2\right)\left(1+\beta^*S^*\right)\right)^{-1}, \tag{5b}$$

where $\tau^* = \frac{V\mu_{\max}}{F}, X_0^* = \frac{X_0}{\alpha K_S}, S_0^* = \frac{S_0}{K_S}, I = \frac{K_S}{K_I}, \beta^* = \frac{\beta K_S}{\alpha}$.

The dimensionless equations have five parameters which are $S_0^*, X_0^*, \beta^*, \tau^*$ and I. In this study, the case of sterile feed is assumed which means $X_0 = 0$ and hence, $X_0^* = 0$. The dimensionless model now has four parameters known as bifurcation parameters since the value of each parameter might change the behaviour of the chemostat system. The dimensionless residence time (τ^*) is the primary bifurcation parameter while the dimensionless initial substrate concentration (S_0^*) is the secondary bifurcation parameter. The dimensionless yield coefficient (β^*) and inhibition constant (I) are third and fourth bifurcation parameters, respectively. However, the value for β^* and I are determined based on the microbial system and hence they are not 'tunable' parameters.

3. Results

The stability and bifurcation analysis of the chemostat model with Andrews growth model and variable yield coefficient has been carried out to identify the dynamical behaviour of microbial in the chemostat. The steady state solutions of the model with their stability and the bifurcation point have been determined.

3.1. Steady state solutions of the chemostat model

The steady state solutions of the dimensionless chemostat model are obtained by letting equation (5a) and equation (5b) equal to zero. There are three steady state solutions of the dimensionless chemostat model which represents the washout and no washout condition in the chemostat. The steady state solutions are given by

i) Washout

$$\left(S^*, X^*\right) = \left(S_0^*, 0\right), \tag{6}$$

ii) No washout

$$\left(S_1^*, X_1^*\right) = \left(\left(-\left(1-\tau^*\right) - \left(\left(\tau^*-1\right)^2 - 4I\right)^{1/2}\right)(2I)^{-1}, X_1^*\right), \tag{7a}$$

$$X_1^* = \left(2I^2\right)^{-1}\begin{bmatrix} I\left(1+2IS_0^* + \left(\left(\tau^*-1\right)^2-4I\right)^{1/2} - \tau^*\right) + \beta^*\left(\tau^*-1\right)\left(1-\tau^* + \left(\left(\tau^*-1\right)^2-4I\right)^{1/2}\right) \\ -\beta^* I\left(-2+S_0^* + S_0^*\left(\left(\tau^*-1\right)^2-4I\right)^{1/2} - S_0^*\tau^*\right) \end{bmatrix}, \tag{7b}$$

$$\left(S_2^*, X_2^*\right) = \left(\left(-\left(1-\tau^*\right) + \left(\left(\tau^*-1\right)^2 - 4I\right)^{1/2}\right)(2I)^{-1}, X_2^*\right), \tag{8a}$$

$$X_2^* = \left(2I^2\right)^{-1}\begin{bmatrix} I\left(1+2IS_0^* - \left(\left(\tau^*-1\right)^2 - 4I\right)^{1/2} - \tau^*\right) - \beta^*\left(\tau^*-1\right)\left(\tau^*-1+\left(\left(\tau^*-1\right)^2-4I\right)^{1/2}\right) \\ +\beta^* I\left(2 - S_0^* + S_0^*\left(\left(\tau^*-1\right)^2-4I\right)^{1/2} + S_0^*\tau^*\right) \end{bmatrix}. \quad (8b)$$

The washout steady state solution as in equation (6) is not physically meaningful since the cell mass concentration is always zero. Hence, further analysis is focused on the no washout steady state solutions, equations (7) and equations (8). The substrate component of the steady state solutions can be defined if $\tau^* \geq 1+2\sqrt{I}$ and the cell mass component is non-negative when the conditions shown in table 1 is satisfied.

Table 1. Conditions for non-negative cell mass concentration of the steady state solutions, provided $\beta > 0$ and $S_0^* > 0$.

Steady State Solution	If $0 < I \leq \frac{1}{\left(S_0^*\right)^2}$	If $I > \frac{1}{\left(S_0^*\right)^2}$
$\left(S_1^*, X_1^*\right)$	$\tau^* \geq IS_0^* + 1 + \left(S_0^*\right)^{-1}$	$\tau^* \geq 1+2\sqrt{I}$,
$\left(S_2^*, X_2^*\right)$.	–	$1+2\sqrt{I} \leq \tau^* \leq IS_0^* + 1 + \left(S_0^*\right)^{-1}$

3.2. Stability of the steady state solutions

The stability of the steady state is determined by finding the Jacobian matrix, determinant, trace and eigenvalues of the dimensionless equation i.e., equation (5a) and equation (5b). The steady state is stable if the trace is negative, the determinant is positive, and the eigenvalues are negative.

3.2.1. Stability of washout steady state solution

The Jacobian matrix (J), determinant (Det), trace (Tr), and eigenvalues (λ) for washout steady state, equation (3) are obtained as follows

$$J = \begin{pmatrix} -\frac{1}{\tau^*} & \frac{-S_0^*}{\left(1+\beta^* S_0^*\right)\left(1+S_0^*+I\left(S_0^*\right)^2\right)} \\ 0 & \frac{S_0^*}{\left(1+S_0^*+I\left(S_0^*\right)^2\right)} - \frac{1}{\tau^*} \end{pmatrix}, \quad (9)$$

$$Det = \left(1-\left(S_0^*\tau^*\right)\left(1+S_0^*+I\left(S_0^*\right)^2\right)^{-1}\right)\left(\tau^*\right)^{-1}, \quad (10)$$

$$Trace = S_0^*\left(1+S_0^*+I\left(S_0^*\right)^2\right)^{-1}-\frac{2}{\tau^*}, \tag{11}$$

$$\lambda_1=-\frac{1}{\tau^*}, \qquad \lambda_2=-\left(1+S_0^*+I\left(S_0^*\right)^2-S_0^*\tau^*\right)\left(\tau^*+S_0^*\tau^*+I\left(S_0^*\right)^2\tau^*\right)^{-1}. \tag{12}$$

By reducing equation (10), equation (11) and equation (12), the washout steady state solution is stable if the following condition is satisfied

$$\tau^* < IS_0^*+1+\left(S_0^*\right)^{-1}. \tag{13}$$

Therefore, the dimensionless residence time (τ^*) should always be more than $IS_0^*+1+\frac{1}{S_0^*}$ to make sure that the steady state is not stable and the washout situation does not occur in the chemostat.

3.2.2. Stability of no washout steady state solutions

There are two no washout steady state solutions which are, equation (4) and equation (5). The Jacobian matrix for both steady state solutions are written as

$$J=\begin{pmatrix} J_{11} & J_{12} \\ J_{21} & 0 \end{pmatrix}, \tag{14}$$

where

$$J_{11}=-\frac{1}{\tau^*}+\frac{\left(-1+I\left(S_i^*\right)^2+\beta^*\left(S_i^*\right)^2\left(1+2IS_i^*\right)X_i^*\right)}{\left(1+\beta^*S_i^*\right)^2\left(1+S_i^*+I\left(S_i^*\right)^2\right)}, \tag{15}$$

$$J_{12}=\frac{-S_i^*}{\left(1+\beta^*S_i^*\right)\left(1+S_i^*+I\left(S_i^*\right)^2\right)}, \tag{16}$$

$$J_{21}=\frac{X_i^*-I\left(S_i^*\right)^2X_i^*}{\left(1+S_i^*+I\left(S_i^*\right)^2\right)}, \tag{17}$$

for $i=1,2$. From the matrix, these steady states will only be stable if trace, $Tr=J_{11}<0$ and determinant, $Det=-J_{12}J_{22}>0$. It is found that the no washout steady state solutions, equation (7) and equation (8) are stable if the following condition is satisfied

$$\tau^* > IS_0^*+1+(S_0^*)^{-1}. \tag{18}$$

However, the second steady state solution, equations (8) will only be positive for $1+2\sqrt{I}<\tau^*\le IS_0^*+1+(S_0^*)^{-1}$, as mentioned in table 1. Hence, it can be concluded that the steady state

(S_2^*, X_2^*) is always physical unmeaningful and the steady state (S_1^*, X_1^*) is always stable when the dimensionless residence time satisfy the condition as in equation (18). The phase plane diagrams of the steady state solutions are plotted by considering two different values of dimensionless residence time $(\tau^* = 1,3)$ to illustrate the stability of the steady state solutions. The initial substrate concentration (S_0^*) is assumed to be 2 and the constants are assumed to be $\beta^* = 5.43, I = 0.08$ [18,22,23]. Figure 1 shows the washout steady state is stable since the dimensionless residence time is less than $IS_0^* + 1 + (S_0^*)^{-1}$ while, figure 2 shows the no washout steady state (S_1^*, X_1^*) is stable since the dimensionless residence time is more than $IS_0^* + 1 + (S_0^*)^{-1}$.

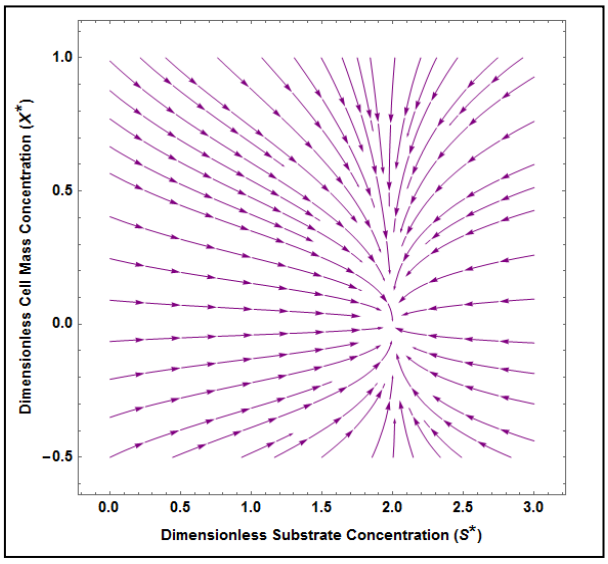

Figure 1. Phase Plane Diagram of the steady state solutions $(\tau^* = 1)$

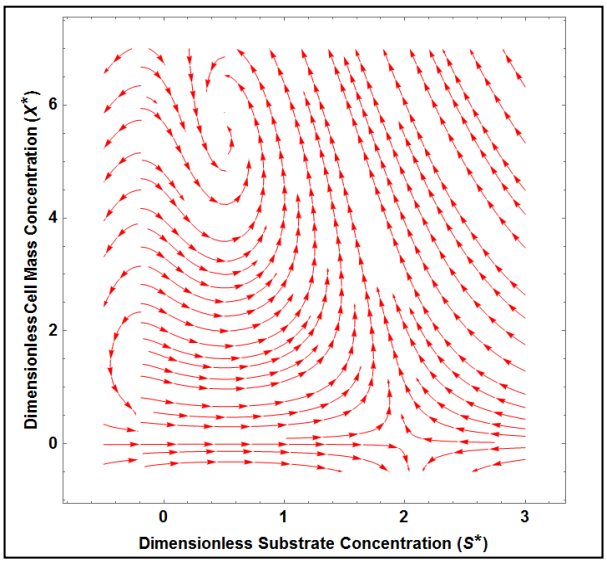

Figure 2. Phase plane diagram of the steady state solutions $(\tau^* = 3)$

3.3. Bifurcation analysis of the no washout steady state solutions

According to Gray and Roberts [24], the conditions for Hopf bifurcation occurs is when the trace is zero, $J_{11}J_{22} = 0$ and the determinant is positive, $J_{11}J_{22} - J_{12}J_{21} > 0$. Previously, we found that the determinant will always be positive when $\tau^* > IS_0^* + 1 + \left(S_0^*\right)^{-1}$. Hence, the bifurcation points can be determined by letting the trace equal to zero which can be written as

$$H(\tau^*) = -\frac{1}{\tau^*} + \frac{\left(-1 + I\left(S_1^*\right)^2 + \beta^*\left(S_0^*\right)^2\left(1 + 2IS_1^*\right)X_1^*\right)}{\left(1 + \beta^* S_1^*\right)^2\left(1 + S_1^* + I\left(S_1^*\right)^2\right)} = 0. \tag{19}$$

The value of residence time at which bifurcation occurs can be found by finding the roots of equation (19). For instance, by substituting $\beta^* = 5.25, I = 0.08$ and $S_0^* = 5$ into equation (19) we get the residence time $\tau^* = 1.64, 2.86$. This means there are bifurcation occur at $\tau^* = 1.64$ and $\tau^* = 2.86$. However, the initial substrate concentration, S_0^* is also a bifurcation parameter. It is important to find the degenerate

Hopf bifurcation point where the two Hopf points are annihilating each other. A degenerate Hopf bifurcation occurs when the following conditions are satisfied

$$H(\tau^*) = 0, \tag{20}$$

$$\frac{dH}{d\tau^*} = 0. \tag{21}$$

The degenerate Hopf bifurcation is obtained by substituting equation (19) into equation (20) and equation (21) which can be written as

$$\left(S_0^*, \tau^*\right) = \left(3.46, 2.20\right), \tag{22}$$

when $\beta^* = 5.25$ and $I = 0.08$. Hence, natural oscillations occur either when $S_0^* < 3.46$ or $S_0^* > 3.46$.

3.3.1. Numerical results

The steady state diagrams of dimensionless cell mass concentration against dimensionless residence time in figure 3 are plotted to determine the existence of natural oscillation for three different values of initial substrate concentrations $(S_0^* = 5,\ 2,\ 0.05)$. The solid lines in the diagrams represents the stable steady state solutions while the dashed lines represents the unstable steady state solutions. Meanwhile, the orange line represents the washout steady state, and the blue and red line represents the no washout steady state, X_1^* and X_2^*, respectively. The dashed black line represents the stable periodic solutions. In figure 3(a), there are two Hopf points that changes the stability of the system while in figure 3(b) and 3(c), no Hopf points is identified and no periodic solutions arise. Therefore, the natural oscillation of microbial population (periodic solutions) occurs when the initial substrate concentration is more than 3.46 ($S_0^* > 6.1$ g/L) for $\beta^* = 5.25$ and $I = 0.08$. The parameter region that can generates the oscillation has been illustrated in figure 4. The unfolding diagram shows the Hopf bifurcation locus and the degenerate Hopf point when $\beta^* = 5.25$ and $I = 0.08$.

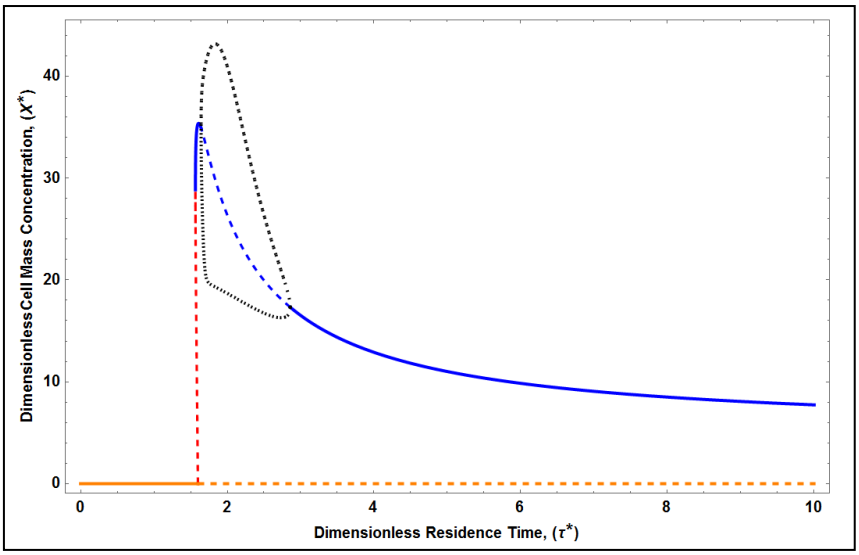

Figure 3(a). Dimensionless steady state solutions (X^*) against dimensionless residence time (τ^*) when $S_0^* = 5$.

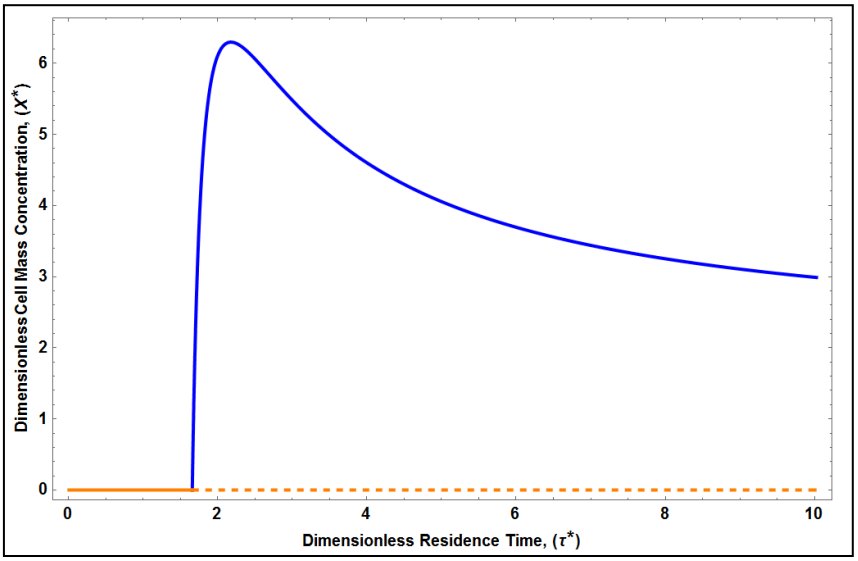

Figure 3(b). Dimensionless steady state solutions (X^*) against dimensionless residence time (τ^*) when $S_0^* = 2$.

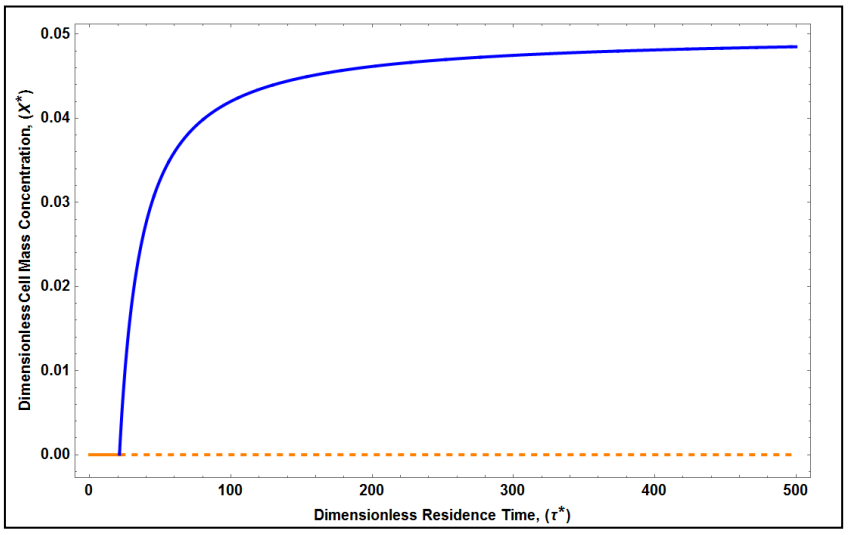

Figure 3(c). Dimensionless steady state solutions (X^*) against dimensionless residence time (τ^*) when $S_0^* = 0.05$.

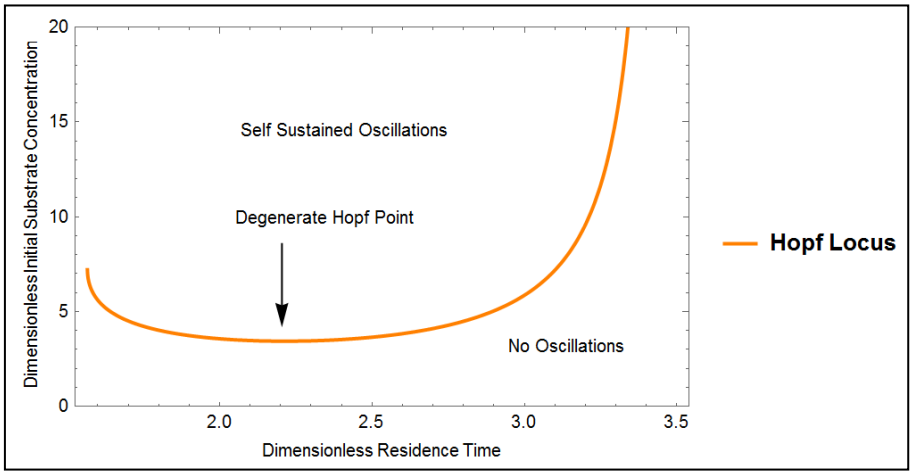

Figure 4. Unfolding diagram showing Hopf bifurcation locus for $\beta^* = 5.25, I = 0.08$

3.4. Condition for maximization of cell mass in the chemostat

Next, in order to determine if there is a residence time at which cell mass concentration is maximised, we let

$$\frac{dX_i^*}{dt^*} = 0, \qquad \text{for } i = 1,2, \tag{23}$$

and the maximum residence time is

$$\tau_{\max}^* = \left(I - 2\beta^* - 2I\beta^* S_0^* + 4\left(\beta^*\right)^2 + 2S_0^*\left(\beta^*\right)^2 + I\left(\beta^*\right)^2\left(S_0^*\right)^2\right)\left(2\beta^*\left(\beta^* S_0^* - 1\right)\right)^{-1}, \tag{24}$$

where $\beta^* S_0^* > 1$. Hence, the steady state diagram of cell mass concentration (X^*) against residence time (τ^*) will have a local maximum at point

$$\left(\tau^*, S_i^*, X_i^*\right) = \left(\tau_{\max}^*, S_{i(\max)}^*, X_{i(\max)}^*\right), \qquad \text{for } i = 1,2, \tag{25}$$

where

$$S_{1(\max)}^* = 4\left(I\left(S_0^* - \frac{1}{\beta^*}\right) + \frac{4\beta^*}{S_0^*\beta^* - 1} + \left(\frac{\left(I\left(S_0^*\beta^* - 1\right)^2 - 4\left(\beta^*\right)^2\right)^2}{\left(\beta^*\right)^2\left(S_0^*\beta^* - 1\right)^2}\right)^{1/2}\right)^{-1}, \tag{26}$$

$$X^*_{1(\max)} = \frac{1}{8\beta^*} + \frac{\beta^*}{I} + \frac{S_0^*}{8}\left(6 + S_0^*\beta^*\right) - \frac{\left(S_0^*\beta^* - 1\right)}{8I}\left(\frac{\left(I\left(S_0^*\beta^* - 1\right)^2 - 4\left(\beta^*\right)^2\right)^2}{\left(\beta^*\right)^2\left(S_0^*\beta^* - 1\right)^2}\right)^{1/2}$$
$$+ \frac{\left(\beta^*\right)^2}{2I^2\left(S_0^*\beta^* - 1\right)^2}\left(-4\beta^* + \left(S_0^*\beta^* - 1\right)\left(\frac{\left(I\left(S_0^*\beta^* - 1\right)^2 - 4\left(\beta^*\right)^2\right)^2}{\left(\beta^*\right)^2\left(S_0^*\beta^* - 1\right)^2}\right)^{1/2}\right), \tag{27}$$

$$S^*_{2(\max)} = 4\left(I\left(S_0^* - \frac{1}{\beta^*}\right) + \frac{4\beta^*}{S_0^*\beta^* - 1} - \left(\frac{\left(I\left(S_0^*\beta^* - 1\right)^2 - 4\left(\beta^*\right)^2\right)^2}{\left(\beta^*\right)^2\left(S_0^*\beta^* - 1\right)^2}\right)^{1/2}\right)^{-1}, \tag{28}$$

$$X^*_{2(\max)} = \frac{1}{8\beta^*} + \frac{\beta^*}{I} + \frac{S_0^*}{8}\left(6 + S_0^*\beta^*\right) + \frac{\left(S_0^*\beta^* - 1\right)}{8I}\left(\frac{\left(I\left(S_0^*\beta^* - 1\right)^2 - 4\left(\beta^*\right)^2\right)^2}{\left(\beta^*\right)^2\left(S_0^*\beta^* - 1\right)^2}\right)^{1/2}$$
$$+ \frac{\left(\beta^*\right)^2}{2I^2\left(S_0^*\beta^* - 1\right)^2}\left(-4\beta^* + \left(S_0^*\beta^* - 1\right)\left(\frac{\left(I\left(S_0^*\beta^* - 1\right)^2 - 4\left(\beta^*\right)^2\right)^2}{\left(\beta^*\right)^2\left(S_0^*\beta^* - 1\right)^2}\right)^{1/2}\right). \tag{29}$$

For instance, when the dimensionless initial subtrate concentration, S_0^* is 2 ($\beta^* S_0^* > 1,$) the cell mass is maximised when the dimensionless residence time, $\tau^*_{\max}$ is 2.18 as shown in figure 3(b). The maximum cell mass concentration, $X^*_{1(\max)}$ is 6.30 and $X^*_{2(\max)}$ is -868.85 which is physically unmeaningful. This means that if the condition $\beta^* S_0^* > 1,$ is satisfied, the cell mass concentration will be maximised at a finite residence time, $\tau^*_{\max}$. If $\beta^* S_0^* < 1,$ then the value of $\tau^*_{\max}$ is negative and the corresponding value of X^* is non-physical. Hence, the steady-state solutions are maximised at an infinite residence time where

$$\lim_{\tau\to\infty} X^*_{1(\max)} = S_0^* \tag{30}$$

$$\lim_{\tau\to\infty} X^*_{2(\max)} = -\infty \tag{31}$$

This is shown in figure 3(c), where the value of S_0^* is 0.05 and the cell mass concentration is maximized at an infinite residence time with $X^*_{1(\max)}$ is approaching 0.05.

4. Conclusion

In this study, the chemostat model with Andrews growth model and variable yield coefficient has been investigated to study the dynamical behaviour of microbial in a chemostat. There are three steady

state solutions found which represents the washout and no washout situations in the chemostat. The conditions at which washout and no washout solutions intersect and exchange stability is given by $\tau^* = IS_0^* + 1 + (S_0^*)^{-1}$. The conditions needed to have positive no washout steady state solutions, are obtained as in table 1. The condition that generate oscillation of microbial in a chemostat has been identified for a given value of β^* and I. The initial substrate concentration (S_0) should be more than 6.1 g/L for generating the oscillation in the chemostat. The parameter range to generate the oscillation in the chemostat has been illustrated in figure 4. Besides that, the requirement to maximize the cell mass concentration in the chemostat has been determined. If $\beta^* S_0^* > 1$, there exist a dimensionless residence time $(\tau_{\max}^*)$, equation (24) that maximize the cell mass concentration $(X_{\max}^*)$, given by equation (27) and equation (29). If $\beta^* S_0^* < 1$, the steady-state solutions are maximised at an infinite residence time where $X_{1(\max)}^* = S_0^*$ and $X_{2(\max)}^* = -\infty$.

Acknowledgments
We would like to express our deepest appreciation for the financial support provided by the Universiti Tun Hussein Onn Malaysia, through grant Tier 1 H076.

References

[1] Monod J 1949 The growth of bacterial cultures *Annu. rev. microbiol.* **3** 371-94
[2] Tessier G 1936 Les lois quantitatives de la croissance *Ann. Physiol. Physiochimie Biol.* **12**, 527–573
[3] Contois D 1959 Kinetics of bacterial growth: Relationship between population density and specific growth rate of continuous cultures *J. Gen. Microbiol.* **21** 40–50
[4] Andrews J F 1968 A mathematical model for the continuous culture of microorganisms utilizing inhibitory substrates *Biotechnol. Bioeng.* **10** 707–723
[5] Abdi N, Hocine G, Tazdait D, Lounici A, Pauss A and Mameri N 2013 Comparison of different models of substrate inhibition in aerobic batch biodegradation of malathion *Turkish J. Eng. Env. Sci.* **37**, 221–230
[6] Costa F and Quintelas C 2012 Kinetics of biodegradation of diethylketone by Arthrobacter viscosus *Biodegrad.* **23** 81-92
[7] Economou C N, Aggelis G, Pavlou S and Vayenas D V 2011 Modeling of single-cell oil production under nitrogen-limited and substrate inhibition conditions *Biotechnol. Bioeng.* **108**, 1049–1055
[8] Goudar C T, Ganji S H, Pujar B G and Strevett K A 2000 Substrate inhibition kinetics of phenol biodegradation *Water Environ. Res.* **72** 50–55
[9] Halmi M I, Shukor M S and Shukor M Y Evaluation of several mathematical models for fitting the growth and kinetics of the catechol-degrading Candida parapsilopsis : Part 2 *J. Env.Bioremed.* **2** 53–57
[10] Krishnan J, Kishore A A, Suresh A, Murali A K and June M 2017 Biodegrdation kinectics of Azo Dye Mixture : substrate inhibition modeling *Res. J. Pharm. Biol. Chem. Sci.* 8 365-375
[11] Rozich A F and Gaudy A F 1985 Response of phenol-acclimated activated sludge process to quantitative shock loading *J. (Water Pollut. Control Fed.)* **57** 795–804
[12] Sokol W 1987 Oxidation of an inhibitory substrate by washed cells (oxidation of phenol by Pseudomonas putida) *Biotechnol. Bioeng.* **30** 921–927
[13] Tan Y, Wang Z X and Marshall K C 1996 Modeling substrate inhibition of microbial growth *Biotechnol. Bioeng.* **52** 602–608
[14] Tang W T and Fan L S 1987 Steady state phenol degradation in a draft-tube, gas-liquid-solid fluidized-bed bioreactor *J. Am. Inst. Chem. Eng.* 33 239–249

[15] Dorofeev A, Glagolev M, Bondarenko T and Panikov N 1992 Observation and ex- planation of the unusual growth-kinetics of Arthrobacter-globiformis *Microbiol.* 61 24–31
[16] Lee I H, Fredrickson A G and Tsuchiya H M 1976 Damped oscillations in continuous culture of Lactobacillus plantarum *J. Gen. Microbiol.* **93** 204–8
[17] Alqahtani R T, Nelson M I and Worthy A L 2012 Analysis of a chemostat model with variable yield coefficient : Contois kinetics *ANZIAM J.* **53** 155–171
[18] Nelson M I and Sidhu H S 2005 Analysis of a chemostat model with variable yield coefficient *J. Math. Chem.* **38** 605–615
[19] Alqahtani R T, Nelson M I and Worthy A L 2015 Analysis of a chemostat model with variable yield coefficient and substrate inhibition : Contois Growth Kinetics *Chem. Eng. Commun.* **202** 332–344
[20] Nelson M I and Sidhu H S 2007 Reducing the emission of pollutants in food processing wastewaters *Chem. Eng. Process. Process Intensif.* **46** 429–436
[21] Nelson M I and Sidhu H S Analysis of a chemostat model with variable yield coefficient: Tessier kinetics *J. Math. Chem.* **46** 303–321
[22] Balakrishnan A and Yang R Y K 2002 Self-forcing of a chemostat with self-sustained oscillations for productivity enhancement *Chem. Eng. Commun.* **189** 1569–1585
[23] Yang R Y K and Su J 1993 Improvement of chemostat performance via nonlinear oscillations *Bioprocess Eng.* **9** 97–102
[24] Gray B F and Roberts M J 1988 A method for the complete qualitative analysis of two coupled ordinary differential equations dependent on three parameters *Proc. R. Soc. A Math. Phys. Eng. Sci.*, **416** 361